Interface focus

J. R. Soc. Interface (2010) **7**, S403–S410
doi:10.1098/rsif.2010.0134.focus
Published online 26 May 2010

Needle-shaped polymeric particles induce transient disruption of cell membranes

Nishit Doshi and Samir Mitragotri*

Department of Chemical Engineering, University of California, Santa Barbara, CA 93106, USA

Nano- and microparticles of various shapes have recently been introduced for various drug-delivery applications. Shape of particles has been shown to have an impact on various processes including circulation, vascular adhesion and phagocytosis. Here, we assess the role of particle geometry and surface chemistry in their interactions with cell membranes. Using representative particles of different shape (spheres, elongated and flat particles), size (500 nm–1 μm) and surface chemistry (positively and negatively charged), we evaluated the response of endothelial cells to particles. While spherical and elliptical disc-shaped particles did not have an impact on cell spreading and motility, needle-shaped particles induced significant changes in the same. Further studies revealed that needle-shaped particles induced disruption of cell membranes as indicated by the release of lactate dehydrogenase and uptake of extracellular calcein. The effect of needle-shaped particles on cells was transient and was reversed over a time period of 1–48 h depending on particle parameters.

Keywords: nanotoxicology; toxicity; drug delivery; shape; nanotube; nanoparticle

1. INTRODUCTION

Designing polymeric carriers for drug delivery has been a topic of great interest for more than two decades (Farokhzad & Langer 2006; Doshi & Mitragotri 2009). While the versatility of polymeric carriers offers numerous advantages including protection from degradation (Soppimath *et al.* 2001), targeted delivery (Langer 1998) and controlled release (Uhrich *et al.* 1999), their rapid clearance from the body and low targeting efficiency limit their applications (Allen & Cullis 2004; Owens & Peppas 2006). Consequently, extensive efforts have been focused on optimization of physical and chemical properties of carriers to accentuate their efficacy (Alexis *et al.* 2008; Mitragotri & Lahann 2009). Towards this end, carriers of several sizes ranging from a few nanometres to several micrometres have been used (Brannon-Peppas 1995; Brigger *et al.* 2002). Surface chemistry of particles has also been extensively engineered (Moghimi *et al.* 2001). Hydrophilic polymers such as polyethylene glycol and their variants have been used to avoid immune recognition of carriers and moieties such as peptides (Ruoslahti 2002; Sugahara *et al.* 2009) and antibodies (Sudimack & Lee 2000) have been used to facilitate target-specific drug delivery. More recently, physical design parameters such as carrier shape (Champion *et al.* 2007*a*,*b*), mechanical flexibility (Beningo & Wang 2002), surface texture (Mitragotri & Lahann 2009) and compartmentalization (Roh *et al.* 2005) have been introduced to further enhance carrier effectiveness.

A wide variety of non-spherical shapes including ellipsoids, discs, cubes, cylinders, hemispheres, cones and other complex shapes such as filovirus-mimicking filamentous particles and red blood cell-like binconcave discoids have been designed using a variety of fabrication techniques and shown to have an impact on biological processes associated with therapeutic delivery (Geng *et al.* 2007; Canelas *et al.* 2009; Doshi & Mitragotri 2009; Doshi *et al.* 2009; Enayati *et al.* 2009). The importance of particle geometry in transport through the vasculature (Decuzzi *et al.* 2009), circulation half life (Geng *et al.* 2007), targeting efficiency (Park *et al.* 2008), phagocytosis (Champion & Mitragotri 2006), endocytosis (Gratton *et al.* 2008; Muro *et al.* 2008) and subsequent intracellular transport (Yoo *et al.* 2009) has been recently established. These studies have demonstrated that particle shape is indeed a key design parameter of drug-delivery carriers.

Here, we study the interactions of particles of three different geometries with endothelial cells. Our studies show that particles of all geometries, in general, were not toxic to cells; however, needle-shaped particles induced transient disruption of cell membranes.

*Author for correspondence (samir@engineering.ucsb.edu).

One contribution to a Theme Supplement 'Scaling the heights—challenges in medical materials: an issue in honour of William Bonfield, Part I. Particles and drug delivery'.

Received 5 March 2010
Accepted 5 May 2010

2. MATERIAL AND METHODS

2.1. Particles

Polystyrene particles with yellow green fluorescence of different sizes and shapes were used to study interactions with endothelial cells. Spheres of two different sizes 0.5 ± 0.012 μm and 1 ± 0.01 μm were purchased from Polysciences (Warrington, PA, USA). Needle- and elliptical disc-shaped particles were fabricated by stretching the spheres using the film stretching method described in Champion *et al.* (2007*a*,*b*). For needles, the spheres were stretched in oil at 120°C, whereas for elliptical discs, the stretching was carried out in toluene at room temperature. Positively charged needles were fabricated by covalently conjugating polyethyleneimine (PEI) to carboxylate modified polystyrene needles using the carbodiimide method (data sheet no. 238 C, Polysciences) with slight modifications. Carboxylate modified needles were prepared by stretching the corresponding spheres using the film stretching method.

2.2. Cells

Murine endothelial cells bEnd.3 were a kind gift from Dr B. Engelhardt, Max-Planck-Institute, Bad Nauheim, Germany; presently at the University of Bern. The cells were cultured with Dulbecco Eagle media (ATCC), which was supplemented with 1 per cent penicillin/streptavidin (Sigma–Aldrich, St Louis, MO, USA) and 10 per cent foetal bovine serum (Invitrogen, Carlsbad, CA, USA). Cells were grown in standard culture conditions (37°C and 5% CO_2).

2.3. Optical and fluorescence microscopy

Cells were cultured overnight in glass bottom delta T dishes (Bioptechs, PA, USA) at a density of around 10^5 cells per dish (3.8 cm^2). The cells were washed with phosphate-buffered saline the next day and the media replaced with HEPES (Sigma–Aldrich, MO, USA) media (DMEM + 25 mM HEPES) to maintain pH in spite of changes in carbon dioxide. Experiments were performed with varying conditions of particle type and concentration and time of incubation. The cells were placed on the stage of an Axiovert 25 microscope (Zeiss, NY, USA), which was fitted with Delta T temperature controller (Bioptechs) that maintained the temperature at 37°C. The cells were observed using a Neo-Fluor oil immersion, 100X, 1.3 NA objective (Zeiss). Brightfield and fluorescent images were taken using a cooled CCD camera ($CoolSnap_{HQ}$, Roper Scientific, GA, USA). Cell surface area (CSA) was calculated by drawing the outline of the cells and measuring the enclosed area in ImageJ image processing software.

2.4. Time-lapse video microscopy

Time-lapse video microscopy was done for a dynamic study of the effect of particles of different shape on cells using Metamorph software (Molecular Devices, PA, USA). The experimental set-up was similar to that described in §2.3. Typically images were taken at an interval of 20 s and compiled into a time-lapse video.

2.5. Lactate dehydrogenase assay

Endothelial cells were seeded at 10^4 cells per well onto a 96-well plate. Particles of different geometry at a concentration of 10^6 per well were applied for 30 min. Twenty-five microlitres of the solution was then transferred to a fresh 96-well plate and mixed with 25 μl of lactate dehydrogenase (LDH) reagent from the CytoTox 96 assay (Promega, Madison, WI, USA) and allowed to react for 30 min in the dark at room temperature. Stop solution (25 μl) was then added to each well, and the absorbance was read at 490 nm. The absorbance was normalized with respect to positive and negative controls. Positive control was cells treated with a lysis solution provided with the assay kit (approx. 0.1% Triton-X100) that would give maximal LDH release, whereas negative control was cells untreated with particles which would result in minimal LDH release. LDH release values range from 0 to 1, with 0 representing minimal LDH release, and 1 indicating maximum LDH release.

2.6. Methyl thiazole tetrazolium assay

Endothelial cells were seeded at 10^4 cells per well onto a 96-well plate. Particles of different geometries at a concentration of 10^6 per well were applied for 30 min. Ten microlitres of reagent from the methyl thiazole tetrazolium (MTT) kit (American Type Culture Collection, Rockville, MD, USA) was applied to each well for 5 h, after which 100 μl of detergent was applied to each well and allowed to incubate in the dark at room temperature for about 40 h. Absorbance was read at 570 nm (MTT dye) and 650 nm (detergent). The contribution of the detergent was subtracted and proliferation potential was calculated. The proliferation potential values range from 0 to 1, with 0 indicating maximum mitochondrial toxicity, and 1 representing high proliferation capacity and healthy cells.

3. RESULTS

Polystyrene particles of three distinct shapes, spheres (S), needles (N, prolate ellipsoids with very high aspect ratio) and elliptical discs (ED), were used in this study. Spheres were purchased as discussed in §2 and other shapes were prepared using methods described in Champion *et al.* (2007*a*,*b*) (figure 1). To assess the impact of size, spheres of two different diameters (500 nm and 1 μm) were used. Needles were also prepared using corresponding spheres. To assess the impact of surface chemistry, spheres (1 μm) and corresponding needles were modified with positively charged PEI in some experiments. In the absence of this modification, all particles possessed a negative charge. A summary of particles used in the study is provided in table 1.

The response of endothelial cells was different for different shapes (100 particles added per cell). Upon exposure to spheres (1 μm), endothelial cells, which generally spread extensively on the substrate, remained spread and did not undergo any notable morphological changes (figure 2*a*). As expected, spheres were

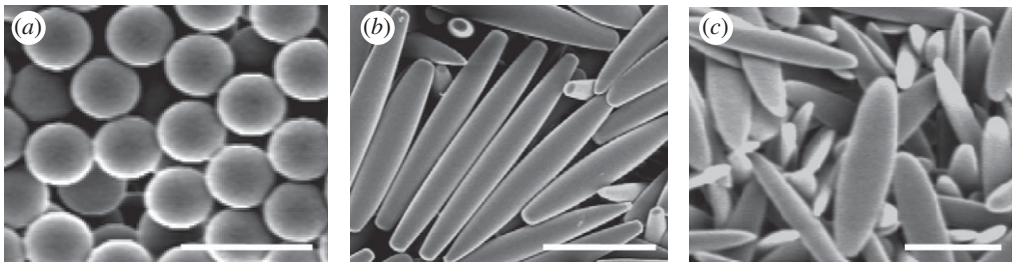

Figure 1. Scanning electron micrographs of particles of different geometry used for the study. (*a*) Spheres, (*b*) needles and (*c*) elliptical discs. Spheres are 1 μm in diameter, whereas needles and elliptical discs are stretched from these spheres. Scale bars, 2 μm.

Table 1. Geometry and surface properties of particles used for this study.

particle geometry	dimension (μm)	surface chemistry
spheres (1 μm)	1	negative (polystyrene)
spheres (1 μm)	1	positive (PEI-coated polystyrene)
needles (from 1 μm spheres)	4.4 × 0.45	negative (polystyrene)
needles (from 1 μm spheres)	4.4 × 0.45	positive (PEI-coated polystyrene)
elliptical discs (from 1 μm spheres)	2.9 × 0.7	negative (polystyrene)
spheres (0.5 μm)	0.5	negative (polystyrene)
needles (from 0.5 μm spheres)	2.1 × 0.23	negative (polystyrene)

internalized by the cells and they eventually accumulated around the nucleus in accordance with the endocytic pathway. Similar behaviour was observed in the case of elliptical discs (figure 2*b*). In contrast, upon exposure to needles, the cells underwent distinct morphological changes. A large population of cells showed contraction in the surface area and some were lifted off from the substrate (figure 2*c*). Moreover, the cells incubated with the needles exhibited higher mobility on the substrate when compared to those incubated with spheres. When observed for sufficiently long times, the contracted cells strived to spread again on the substrate indicating that the contraction is not permanent.

Cellular contractions were quantified in terms of normalized CSA (figure 3*a*). While spheres and elliptical discs induced no significant changes in CSA (approx. 10%), there was a significant drop in the CSA when treated with needles. After 2 h, the average reduction in CSA for cells exposed to needles was approximately 65 per cent. Time-lapse video microscopy was used to follow CSA over 48 h. Exposure to needles induced significant reduction in the number of well-spread cells within 2 h of exposure. However, the cells recovered over time and approached the initial extent of spreading at 48 h (figure 3*b*).

The effect of particles on cells also depended on their size, especially for needles (figure 4*a*). The decrease in CSA was smaller for needles made from 500 nm spheres when compared with that for needles made from 1 μm spheres. The extent of particle stretching (aspect ratio) was maintained constant in both cases to exclusively study the effect of size. Surface chemistry also exhibited a strong impact on cell contraction (figure 4*b*). Positively charged needles exhibited more rapid reduction of CSA when compared with their negatively charged counterparts. They also led to quicker recovery to baseline.

The effect of particles on cells was further quantified using LDH and the MTT assay. While LDH release indicates disruption of cell membranes, the MTT assay measures the metabolic activity of cells. These studies were performed using spheres and needles. Needles induced significantly higher release of LDH from endothelial cells compared with spheres, which induced negligible LDH release (figure 5*a*). MTT assays, on the other hand, revealed no major difference between the needles and spheres, both of which were comparable to cells not exposed to any particles (figure 5*b*).

Application of particles to cells led to intracellular penetration of a concurrently applied fluorescent marker, calcein (figure 6*a*,*b*). However, a major difference was found for spheres and needles. Spheres did not induce a significant impact on cells, which exhibited usual pinocytic internalization of extracellular calcein. This is evident through the appearance of small punctuate intracellular fluorescent spots, which are characteristic of the pinocytic pathway. Exposure to needles, however, induced a different mode of calcein uptake. Diffused calcein was found throughout the cell, indicative of transmembrane calcein uptake. The distinction between the pinocytic and transmembrane uptake of calcein is particularly evident from the insets of figure 6 which show enlarged views of the highlighted sections in the respective main images. There is pinocytic uptake in needle-exposed cells as well. This is expected since transmembrane calcein transport does not preclude pinocytic uptake, especially once the cells are recovered.

4. DISCUSSION

Most therapeutic delivery carriers currently under investigation or in clinical practice are spherical in shape. However, particles of different geometry have recently been shown to perform several delivery functions significantly better than spheres. For example, elongated particles have been shown to

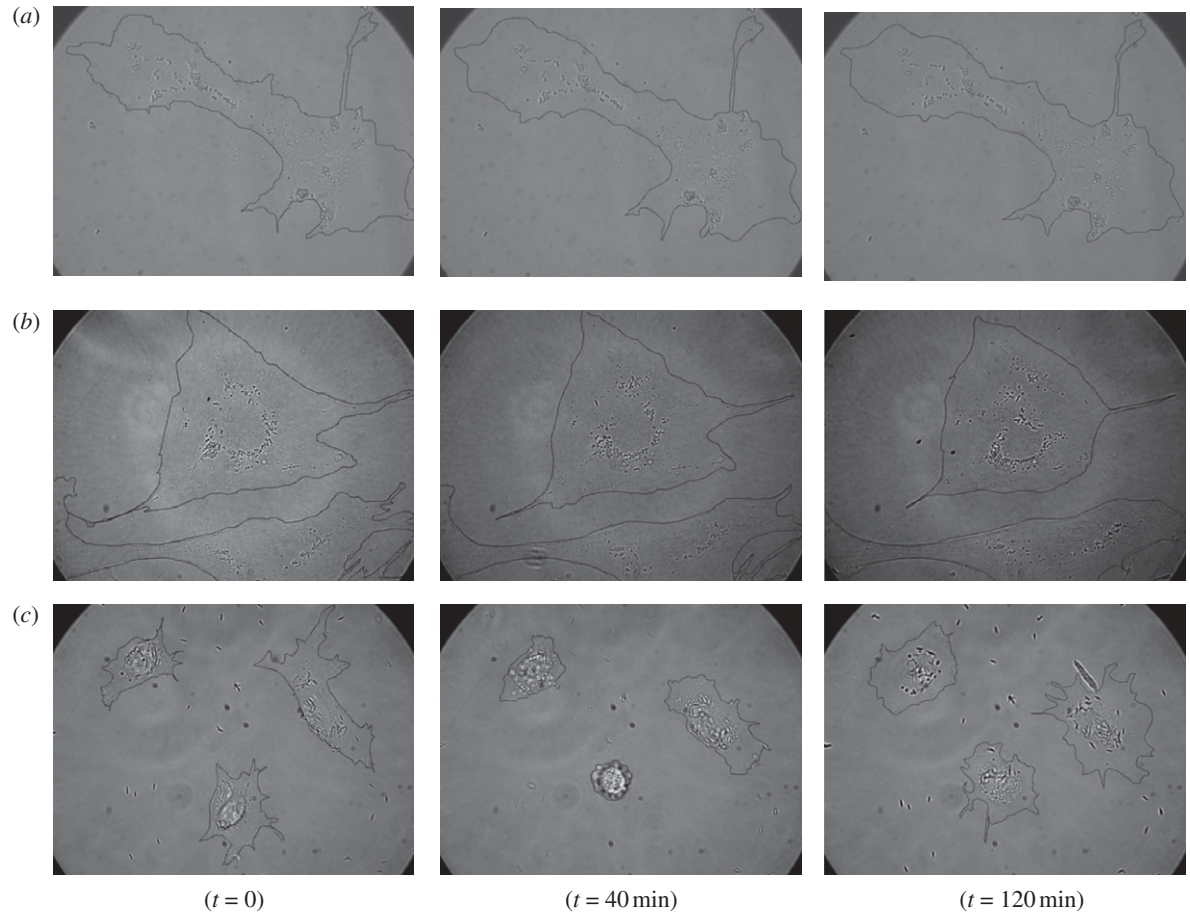

Figure 2. Time-lapse video microscopy images of interaction of particles of different geometry with endothelial cells at different time points: spheres (*a*), elliptical discs (*b*) and needles (*c*). The cells incubated with spheres and elliptical discs do not show significant morphological changes over time, whereas in the case of needles, the cells undergo contraction and re-spread over time. Cell boundaries have been drawn manually as a visual aid.

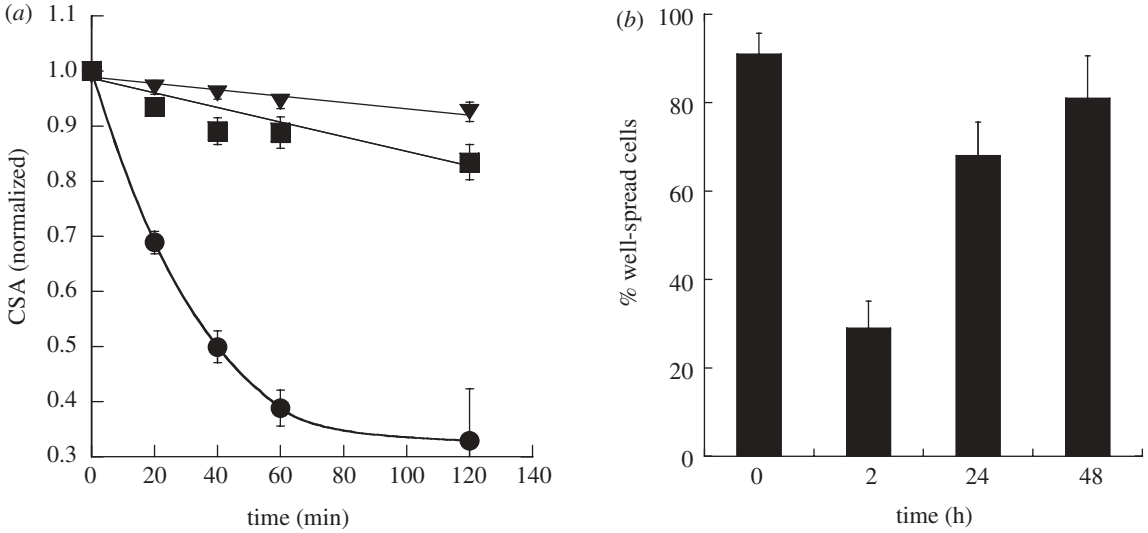

Figure 3. Kinetics of cellular contractions caused by particles of different geometry on endothelial cells. (*a*) Plot of normalized CSA for spheres (squares), elliptical discs (triangles) and needles (circles) against time. Spheres are 1 μm in diameter, whereas needles and elliptical discs are stretched from these spheres. The CSA for spheres and elliptical discs varies at most 15 per cent over a period of 2 h, whereas for needles, the CSA decreases rapidly by more than 65 per cent in 2 h. (*b*) Percentage of well-spread cells before and after the treatment with needles for 2, 24 and 48 h. The percentage of well-spread cells decreases drastically 2 h after incubation with needles; however, the cells recover to the baseline in approximately 48 h.

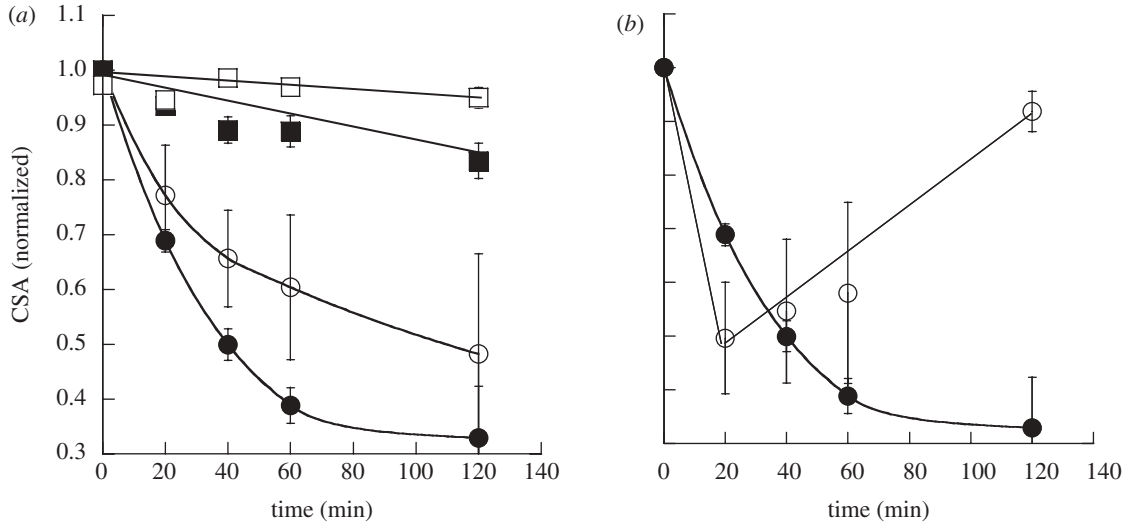

Figure 4. Effect of size and surface chemistry on the kinetics of cellular contractions caused by particles of different shape on endothelial cells. (*a*) Effect of size of particles on normalized CSA. Spheres of two different sizes of 1 μm (filled squares) and 0.5 μm (open squares) and corresponding needles (filled circles and open circles, respectively) stretched from these spheres were used. Large-sized particles showed more drastic effects on endothelial cells. (*b*) Effect of plain needles (filled circles) and positively charged needles (open circles) on normalized CSA. Positively charged particles result in rapid reduction of CSA and rapid recovery compared with plain needles. The lines are drawn to guide the eye.

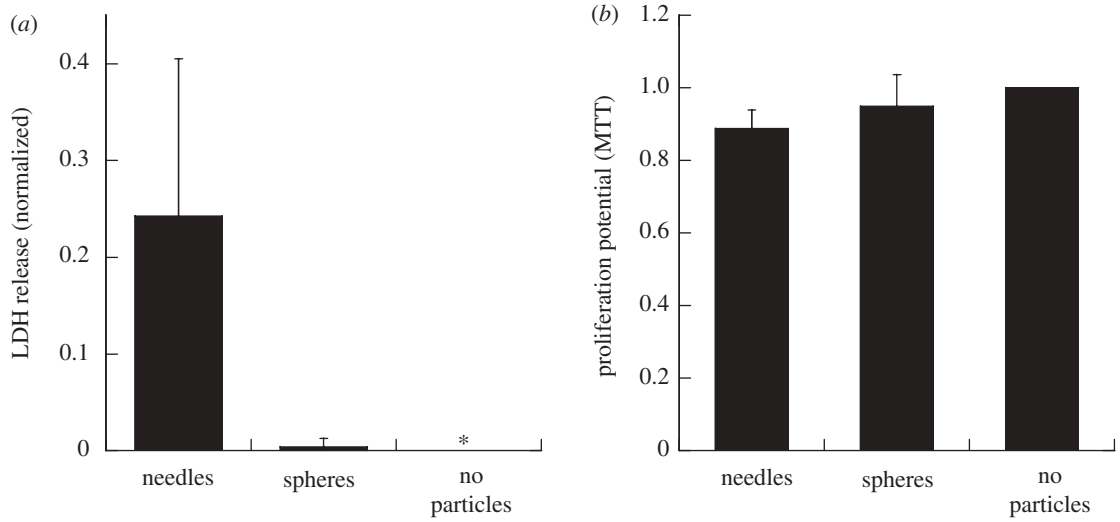

Figure 5. Toxicological assays with particles of different geometry on endothelial cells. (*a*) LDH release from endothelial cells upon interaction with particles of different geometry. One micrometre spheres and needles stretched from these spheres were used for the assay. Needles showed significantly higher LDH release when compared with spheres ($p < 0.01$, $n = 5$). (*b*) Proliferation potential of endothelial cells upon incubation with particles of different geometry as determined by the MTT assay. One micrometre spheres and needles stretched from these spheres were used for the assay. There was no significant difference in the proliferation potential of spheres and needles ($p > 0.05$, $n = 5$) and it was close to negative control.

avoid phagocytosis and remain in circulation for longer times, whereas both elongated and flat particles have been shown to target the diseased site better than their spherical counterparts (Doshi & Mitragotri 2009). As these non-spherical particles become commonplace in drug delivery, their interactions with cells must be understood. Using spheres, needles and elliptical discs, we sought to assess how particles of various geometries interact with endothelial cells. These cells were chosen since endothelium is an important target in drug delivery owing to its role in a number of pathological disorders including inflammation, oxidative stress and thrombosis (Muro *et al.* 2003, 2004).

The response of endothelial cells to particles exhibited a clear dependence on shape. Cells exposed to spheres and elliptical discs did not exhibit departure from their usual behaviour. They remained spread, and endocytozed the particles. Exposure to needles, on the other hand, induced a dramatically different behaviour. Cells exhibited extensive contraction and significantly lower extent of endocytosis was observed. The extent of contraction decreased with a decrease in particle size, whereas the use of positively charged particles resulted in accelerated contraction kinetics; however, both change in size and surface chemistry did not fundamentally change the effect of needles on

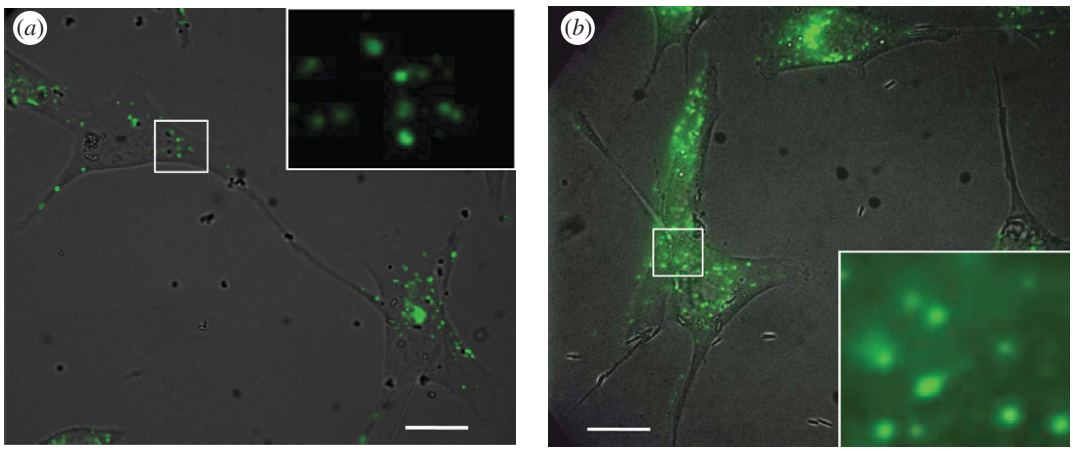

Figure 6. Calcein uptake by endothelial cells incubated with particles of different shapes. The figures show overlaid brightfield and fluorescent images. (*a*) 1 μm spheres. The punctuate fluorescent spots clearly indicate pinocytic uptake of calcein. (*b*) Needles stretched from 1 μm spheres. The diffuse fluorescence of calcein in the cell membrane indicates transmembrane uptake in this case. Scale bar, 20 μm. The insets show enlarged images of sections shown by white rectangles in the main images. The insets show only fluorescent images.

cells. Further experiments that evaluate the effect of charge density and surface potential of particles are required to better understand the effect of surface chemistry. Cellular contraction was transient and the cells recovered over 48 h. Contraction of cells was associated with the release of LDH, which is an exclusively intracellular enzyme and is not released unless membrane integrity is compromised. While cells not exposed to particles or those exposed to spheres did not exhibit LDH release, cells exposed to needles induced detectable LDH release (approx. 0.25, where 1 corresponds to complete membrane disruption by 0.1% Triton X). Particle-induced membrane disruption was also evident from transmembrane delivery of calcein. Upon co-incubation with spheres, calcein was internalized by cells via pinocytic mechanism as revealed by the appearance of punctuate fluorescent spots within the cells. Co-incubation with needles, on the other hand, led to penetration of calcein into cells. Unlike in the case of spheres, calcein was present in a diffuse manner in the cytoplasm. Disruption of cell membranes did not appear to induce noticeable toxicity as assessed by MTT assay.

Intentional transient disruption of cell membranes has been an active area of research in the field of drug delivery. Various methods including electroporation (Canatella *et al.* 2001), ultrasound (Tachibana *et al.* 1999), chemical penetration enhancers (Williams & Barry 2004; Whitehead & Mitragotri 2008) and peptides (Lindgren *et al.* 2000) have been studied to induce transient membrane disruption. However, membrane disruption using polymeric particles is a novel phenomenon. There is evidence in the literature that carbon nanotubes with exceptionally high aspect ratio cause cell permeabilization. For example, carbon nanotubes have been shown to permeabilize endothelial cells, fibroblasts and even microbes such as *Escherichia coli* (Pantarotto *et al.* 2004; Yamawaki & Iwai 2006; Kang *et al.* 2007) in a size-dependent manner (Kang *et al.* 2008). In most cases, increased permeabilization also leads to high toxicity to cells (Klumpp *et al.* 2006; Yamawaki & Iwai 2006; Kang *et al.* 2007). The general consensus is that cytotoxicity of carbon nanotubes is mediated by their physical penetration across the cell membrane resulting in punctured cells (Klumpp *et al.* 2006; Kang *et al.* 2007). This property of carbon nanotubes is also being explored for therapeutic applications (Klumpp *et al.* 2006). The ability of nanotubes to penetrate membranes is also being studied as a potential mediator of inflammation, epithelioid granulomas (microscopic nodules), fibrosis and biochemical/toxicological changes in the lungs (Lam *et al.* 2004, 2006).

The results presented here indicate an interesting scenario where needle-shaped polymeric particles, which possess an aspect ratio higher than spheres but significantly lower than carbon nanotubes, induce transient disruption of cell membranes. The precise extent of membrane disruption is likely to depend on several parameters including size, shape, surface chemistry, particle dose, incubation time and cell type. Like other methods of membrane permeabilization including electroporation and ultrasound, it is likely that excessive disruption may compromise reversibility and lead to cell death. Hence, detailed studies are necessary to fully elucidate the dependence of disruption on key parameters. Through such experiments, one can further engineer particles to enable better control over cell membrane permeabilization. Because of the reversible nature of this phenomenon, polymer particle-mediated membrane penetration may find applications in the delivery of siRNA and other drugs.

5. CONCLUSIONS

The studies reported here demonstrate that particles of different shapes exhibit distinct interactions with cells. While spheres and elliptical discs exhibited minimal interactions with cells other than endocytosis, needle-shaped particles induced membrane disruption and increased cell mobility. Particle size and surface chemistry were found to affect the membrane disruption kinetics. Moreover, the membrane permeability and

cellular toxicity were found to be transient since the morphological changes induced in the cells were seen to revert back with time. The reversible nature of cell membrane permeability can find applications in the delivery of drugs as demonstrated by the delivery of calcein, a model small molecule drug. Further experiments by varying the various dependent parameters will enable better control over membrane permeabilization. These findings have significant implications in developing new methods of drug delivery as well as in understanding the toxicity of particulate matter to cells.

The authors acknowledge financial support from the National Heart Lung and Blood Institute's Program of Excellence in Nanotechnology (1UO1 HL080718). The authors acknowledge Poornima Kolhar for help with experiments and Claudia Gottstein for help with cells.

REFERENCES

Alexis, F., Pridgen, E., Molnar, L. K. & Farokhzad, O. C. 2008 Factors affecting the clearance and biodistribution of polymeric nanoparticles. *Mol. Pharm.* **5**, 505–515. (doi:10.1021/mp800051m)

Allen, T. M. & Cullis, P. R. 2004 Drug delivery systems: entering the mainstream. *Science* **303**, 1818–1822. (doi:10.1126/science.1095833)

Beningo, K. A. & Wang, Y. L. 2002 Fc-receptor-mediated phagocytosis is regulated by mechanical properties of the target. *J. Cell Sci.* **115**, 849–856.

Brannon-Peppas, L. 1995 Recent advances on the use of biodegradable microparticles and nanoparticles in controlled drug delivery. *Int. J. Pharm.* **116**, 1–9. (doi:10.1016/0378-5173(94)00324-X)

Brigger, I., Dubernet, C. & Couvreur, P. 2002 Nanoparticles in cancer therapy and diagnosis. *Adv. Drug Deliv. Rev.* **54**, 631–651. (doi:10.1016/S0169-409X(02)00044-3)

Canatella, P., Karr, J. F., Petros, J. A. & Prausnitz, M. R. 2001 Quantitative study of electroporation-mediated molecular uptake and cell viability. *Biophys. J.* **80**, 755–764. (doi:10.1016/S0006-3495(01)76055-9)

Canelas, D., Herlihy, K. P. & DeSimone, J. M. 2009 Top-down particle fabrication: control of size and shape for diagnostic imaging and drug delivery. *Wiley Interdisc. Rev.: Nanomed. Nanobiotechnol.* **1**, 391–404. (doi:10.1002/wnan.40)

Champion, J. A. & Mitragotri, S. 2006 Role of target geometry in phagocytosis. *Proc. Natl Acad. Sci. USA* **103**, 4930–4934. (doi:10.1073/pnas.0600997103)

Champion, J., Katare, Y. K. & Mitragotri, S. 2007*a* Particle shape: a new design parameter for micro- and nanoscale drug delivery carriers. *J. Control. Rel.* **121**, 3–9. (doi:10.1016/j.jconrel.2007.03.022)

Champion, J. A., Katare, Y. K. & Mitragotri, S. 2007*b* Making polymeric micro- and nanoparticles of complex shapes. *Proc. Natl Acad. Sci. USA* **104**, 11 901–11 904. (doi:10.1073/pnas.0705326104)

Decuzzi, P., Godin, B., Tanaka, T., Lee, S.-Y., Chiappini, C., Liu, X. & Ferrari, M. 2009 Size and shape effects in the biodistribution of intravascularly injected particles. *J. Control. Rel.* **141**, 320–327. (doi:10.1016/j.jconrel.2009.10.014)

Doshi, N. & Mitragotri, S. 2009 Designer biomaterials for nanomedicine. *Adv. Funct. Mater.* **19**, 3843–3854. (doi:10.1002/adfm.200901538)

Doshi, N., Zahr, A. S., Bhaskar, S., Lahann, J. & Mitragotri, S. 2009 Red blood cell-mimicking synthetic biomaterial particles. *Proc. Natl Acad. Sci. USA* **106**, 21 495–21 499. (doi:10.1073/pnas.0907127106)

Enayati, M., Ahmad, Z., Stride, E. & Edirisinghe, M. 2009 Preparation of polymeric carriers for drug delivery with different shape and size using an electric jet. *Curr. Pharm. Biotechnol.* **10**, 600–608. (doi:10.2174/138920109789069323)

Farokhzad, O. & Langer, R. 2006 Nanomedicine: developing smarter therapeutic and diagnostic modalities. *Adv. Drug Deliv. Rev.* **58**, 1456–1459. (doi:10.1016/j.addr.2006.09.011)

Geng, Y., Dalhaimer, P., Cai, S., Tsai, R., Tewari, M., Minko, T. & Discher, D. E. 2007 Shape effects of filaments versus spherical particles in flow and drug delivery. *Nat. Nanotechnol.* **2**, 249–255. (doi:10.1038/nnano.2007.70)

Gratton, S., Ropp, P. A., Pohlhaus, P. D., Luft, J. C., Madden, V. J., Napier, M. E. & DeSimone, J. M. 2008 The effect of particle design on cellular internalization pathways. *Proc. Natl Acad. Sci. USA* **105**, 11 613–11 618. (doi:10.1073/pnas.0801763105)

Kang, S., Pinault, M., Pfefferle, L. D. & Elimelech, M. 2007 Single-walled carbon nanotubes exhibit strong antimicrobial activity. *Langmuir* **23**, 8670–8673. (doi:10.1021/la701067r)

Kang, S., Herzberg, M., Rodrigues, D. F. & Elimelech, M. 2008 Antibacterial effects of carbon nanotubes: size does matter! *Langmuir* **24**, 6409–6413. (doi:10.1021/la800951v)

Klumpp, C., Kosteralos, K., Prato, M. & Blanco, A. 2006 Functionalized carbon nanotubes as emerging nanovectors for the delivery of therapeutics. *Biochim. Biophys. Acta Biomembr.* **1758**, 404–412. (doi:10.1016/j.bbamem.2005.10.008)

Lam, C., James, J. T., McCluskey, R. & Hunter, R. L. 2004 Pulmonary toxicity of single-wall carbon nanotubes in mice 7 and 90 days after intratracheal instillation. *Toxicol. Sci.* **77**, 126–134. (doi:10.1093/toxsci/kfg243)

Lam, C., James, J. T., McCluskey, R., Arepalli, S. & Hunter, R. L. 2006 A review of carbon nanotube toxicity and assessment of potential occupational and environmental health risks. *CRC Crit. Rev. Toxicol.* **36**, 189–217. (doi:10.1080/10408440600570233)

Langer, R. 1998 Drug delivery and targeting. *Nature* (*Lond.*) **392**, 5–10.

Lindgren, M., Hällbrink, M., Prochiantz, A. & Langel, U. 2000 Cell-penetrating peptides. *Trends Pharmacol. Sci.* **21**, 99–103. (doi:10.1016/S0165-6147(00)01447-4)

Mitragotri, S. & Lahann, J. 2009 Physical approaches to biomaterial design. *Nat. Mater.* **8**, 15–23. (doi:10.1038/nmat2344)

Moghimi, S. M., Hunter, A. C. & Murray, J. C. 2001 Long-circulating and target-specific nanoparticles: theory to practice. *Pharmacol. Rev.* **53**, 283–318.

Muro, S., Cui, X., Gajewski, C., Murciano, J.-C., Muzykantov, V. R. & Koval, M. 2003 Slow intracellular trafficking of catalase nanoparticles targeted to ICAM-1 protects endothelial cells from oxidative stress. *Am. J. Physiol. Cell Physiol.* **285**, C1339–C1347. (doi:10.1152/ajpcell.00099.2003)

Muro, S., Koval, M. & Muzykantov, V. 2004 Endothelial endocytic pathways: gates for vascular drug delivery. *Curr. Vasc. Pharmacol.* **2**, 281–299. (doi:10.2174/1570161043385736)

Muro, S., Garnacho, C., Champion, J. A., Leferovich, J., Gajewski, C., Schuchman, E. H., Mitragotri, S. & Muzykantov, V. R. 2008 Control of endothelial targeting and intracellular delivery of therapeutic enzymes by modulating the size and shape of ICAM-1-targeted carriers. *Mol. Ther.* **16**, 1450–1458. (doi:10.1038/mt.2008.127)

Owens III, D. E. & Peppas, N. A. 2006 Opsonization, biodistribution, and pharmacokinetics of polymeric nanoparticles. *Int. J. Pharm.* **307**, 93–102. (doi:10.1016/j.ijpharm.2005.10.010)

Pantarotto, D., Briand, J.-P., Prato, M. & Bianco, A. 2004 Translocation of bioactive peptides across cell membranes by carbon nanotubes. *Chem. Commun.* **2004**, 16–17. (doi:10.1039/b311254c)

Park, J., von Maltzahn, G., Zhang, L., Schwartz, M. P., Ruoslahti, E., Bhatia, S. N. & Sailor, M. J. 2008 Magnetic iron oxide nanoworms for tumor targeting and imaging. *Adv. Mater.* **20**, 1630–1635. (doi:10.1002/adma.200800004)

Roh, K., Martin, D. C. & Lahann, J. 2005 Biphasic Janus particles with nanoscale anisotropy. *Nat. Mater.* **4**, 759–763. (doi:10.1038/nmat1486)

Ruoslahti, E. 2002 Drug targeting to specific vascular sites. *Drug Discov. Today* **7**, 1138–1143. (doi:10.1016/S1359-6446(02)02501-1)

Soppimath, K. S., Aminabhavi, T. M., Kulkarni, A. R. & Rudzinski, W. E. 2001 Biodegradable polymeric nanoparticles as drug delivery devices. *J. Control. Rel.* **70**, 1–20. (doi:10.1016/S0168-3659(00)00339-4)

Sudimack, J. & Lee, R. 2000 Targeted drug delivery via the folate receptor. *Adv. Drug Deliv. Rev.* **41**, 147–162. (doi:10.1016/S0169-409X(99)00062-9)

Sugahara, K., Teesalu, T., Karmali, P., Kotamraju, V., Agemy, L., Girard, O., Hanahan, D., Mattrey, R. & Ruoslahti, E. 2009 Tissue-penetrating delivery of compounds and nanoparticles into tumors. *Cancer Cell* **16**, 510–520. (doi:10.1016/j.ccr.2009.10.013)

Tachibana, K., Uchida, T., Ogawa, K., Yamashita, N. & Tamura, K. 1999 Induction of cell-membrane porosity by ultrasound. *Lancet* **353**, 1409. (doi:10.1016/S0140-6736(99)01244-1)

Uhrich, K., Cannizaro, S. M., Langer, R. S. & Shakesheff, K. M. 1999 Polymeric systems for controlled drug release. *Chem. Rev.* **99**, 3181–3198. (doi:10.1021/cr940351u)

Whitehead, K. & Mitragotri, S. 2008 Mechanistic analysis of chemical permeation enhancers for oral drug delivery. *Pharm. Res.* **25**, 1412–1419. (doi:10.1007/s11095-008-9542-2)

Williams, A. & Barry, B. 2004 Penetration enhancers. *Adv. Drug Deliv. Rev.* **56**, 603–618. (doi:10.1016/j.addr.2003.10.025)

Yamawaki, H. & Iwai, N. 2006 Cytotoxicity of water-soluble fullerene in vascular endothelial cells. *Am. J. Physiol. Cell Physiol.* **290**, C1495–C1502. (doi:10.1152/ajpcell.00481.2005)

Yoo, J., Doshi, N. & Mitragotri, S. 2009 Endocytosis and intracellular distribution of PLGA particles in endothelial cells: effect of particle geometry. *Macromol. Rapid Commun.* **31**, 142–148. (doi:10.1002/marc.200900592)